NMR studies of hydrogen diffusion in the hydrogen-stabilized Laves phase compound C15-Hf Ti_2H_x

2002 J. Phys.: Condens. Matter 14 153

(http://iopscience.iop.org/0953-8984/14/2/303)

INSTITUTE OF PHYSICS PUBLISHING JOURNAL OF PHYSICS: CONDENSED MATTER

J. Phys.: Condens. Matter **14** (2002) 153–164 PII: S0953-8984(02)26635-7

NMR studies of hydrogen diffusion in the hydrogen-stabilized Laves phase compound C15-Hf Ti_2H_x

U Eberle[1], G Majer[1,3], A V Skripov[2] and V N Kozhanov[2]

[1] Max-Planck-Institut für Metallforschung, Heisenbergstr. 1, 70569 Stuttgart, Germany
[2] Institute of Metal Physics, Urals Branch of the Academy of Sciences, Ekaterinburg 620219, Russia

E-mail: majer@nmr.mpi-stuttgart.mpg.de

Received 6 July 2001, in final form 7 November 2001
Published 13 December 2001
Online at stacks.iop.org/JPhysCM/14/153

Abstract

Measurements of the hydrogen diffusivity in the hydrogen-stabilized Laves phase compound C15-Hf Ti_2H_x ($3.9 \leqslant x \leqslant 4.2$) have been performed by means of the pulsed-field-gradient nuclear magnetic resonance (PFG-NMR) between 220 and 500 K. The activation enthalpies for hydrogen diffusion obtained by fitting an Arrhenius expression to the diffusivities measured at a given concentration x are $H_a = 240$ meV ($x = 3.9$), 210 meV ($x = 4.0$) and 235 meV ($x = 4.2$). The proton spin–lattice relaxation rates Γ_1 have been measured on the same samples over wide temperature ranges and at different resonance frequencies. Above about 250 K, the Γ_1 data are well represented by a relaxation model for jumps between tetrahedral [Hf Ti_3] sites. A comparison with the PFG results shows that these jumps correspond to long-range diffusion. At lower temperatures, the Γ_1 data indicate localized motion of hydrogen, presumably within hexagons formed by six tetrahedral [Hf_2Ti_2] sites, which has no effect on the PFG measurements. Similar diffusion mechanisms have been observed previously in C15-$ZrTi_2H_x$ ($x \approx 4$).

1. Introduction

Many intermetallic AB_2 compounds with the C15 structure, so-called cubic Laves phases (space group $Fd\bar{3}m$), form hydrides with large hydrogen contents. In these systems hydrogen atoms occupy two types of tetrahedral interstitial sites, the g-sites surrounded by two A and two B atoms and the e-sites surrounded by one A and three B atoms. There are 12 g-sites and four e-sites per formula unit AB_2. In most C15-AB_2H_x compounds only g-sites are occupied up to $x \approx 2.5$. In these systems generally two processes of hydrogen motion exist: besides fast

[3] Corresponding author.

localized motion of hydrogen within hexagons formed by six g-sites, the long-range diffusion occurs by jumps between adjacent hexagons [1–3]. At higher concentrations hydrogen atoms start to occupy e-sites in addition to the g-sites [4, 5], resulting in an increased hydrogen diffusivity and a reduced effective activation enthalpy H_a for long-range diffusion [6].

Of particular interest are the diffusion mechanisms in those Laves-phase compounds, in which a large fraction of hydrogen atoms occupy e-sites, such as C15-$ZrTi_2H_x$ and C15-$HfTi_2H_x$. The systems Hf–Ti and Zr–Ti form disordered hexagonal close-packed (hcp) alloys. However, the absorption of hydrogen by $ZrTi_2$ and $HfTi_2$ results in the formation of the cubic Laves-phases C15-$ZrTi_2H_x$ ($3 \leqslant x \leqslant 4$) [7] and C15-$HfTi_2H_x$ ($3.5 \leqslant x \leqslant 4.5$) [8]. In both systems the ordering of the host-metal lattice is induced by hydrogen and the hcp alloy is formed again when the hydrogen is removed. According to neutron diffraction measurements on deuterium-stabilized C15-$ZrTi_2D_x$ [7,9] and C15-$HfTi_2D_x$ [10], hydrogen (deuterium) atoms occupy in these compounds, in contrast to most other Laves-phase hydrides, mainly e-sites. At low temperatures the g-site occupancy is negligible, but at room temperature the neutron scattering data yield a g-site occupation probability of about $c_g = 0.07$ in C15-$HfTi_2D_4$ [10] and about $c_g = 0.05$ in C15-$ZrTi_2D_{3.83}$ [9].

Nuclear magnetic resonance (NMR) is a unique technique to study the hydrogen motion in metal hydrides on both macroscopic and microscopic scales. The jump frequency of hydrogen atoms can in principle be obtained from the dipolar contribution to the proton spin–lattice relaxation rate Γ_{1d} by applying an appropriate relaxation model. The pulsed-field-gradient (PFG) spin-echo NMR technique [11, 12], on the other hand, permits direct measurement of the *long-range* diffusivity D. In a series of Laves-phase hydrides, D has been measured by PFG-NMR as a function of temperature and hydrogen concentration [6, 13–16]. Together with information available from Γ_1 measurements, such data permit to distinguish between long-range diffusion and localized motion.

Γ_1 and $\Gamma_{1\rho}$ (rotating frame) data of hydrogen in C15-$ZrTi_2H_x$ have been interpreted in terms of a double-peak distribution of activation enthalpies for hydrogen motion [17]. This approach implies the coexistence of two types of hydrogen motion on different time scales. By direct PFG measurements of hydrogen diffusion in C15-$ZrTi_2H_{3.7}$ it was possible to identify one type of motion as long-range diffusion and the other one as localized motion. Quasi-elastic neutron scattering (QENS) experiments on C15-$ZrTi_2H_{3.9}$ have confirmed the existence of fast localized hydrogen motion in this compound, and, moreover, a very similar behaviour has been found for hydrogen-stabilized C15-$HfTi_2H_x$ ($x = 3.5$ and 4.0) [18]. On the basis of these QENS data, the following microscopic picture of hydrogen motion in hydrogen-stabilized Laves-phase compound has been proposed [18]: most of the hydrogen atoms occupy the nearly completely filled sublattice of e-sites. Transitions between e-sites are likely to occur via at least two intermediate g-sites (cf figure 1). If a hydrogen atom moves to a g-site, it can participate in the fast localized motion over g-site hexagons. The jump back to the e-site sublattice may occur at a different position leading to long-range diffusion.

The present paper reports on NMR studies of hydrogen motion in the hydrogen-stabilized compounds C15-$HfTi_2H_x$ ($x = 3.9$, 4.0 and 4.2) by Γ_1 and PFG measurements. The main goals are to characterize the different types of hydrogen motion and to proof the correctness of the proposed diffusion model. The present results for C15-$HfTi_2H_x$ will be compared with the data for C15-$ZrTi_2H_x$.

2. Experimental details

The preparation of the $HfTi_2H_x$ samples ($x = 3.9$, 4.0 and 4.2) has been described in [8]. According to the x-ray diffraction analysis, all three samples are single phase compounds with

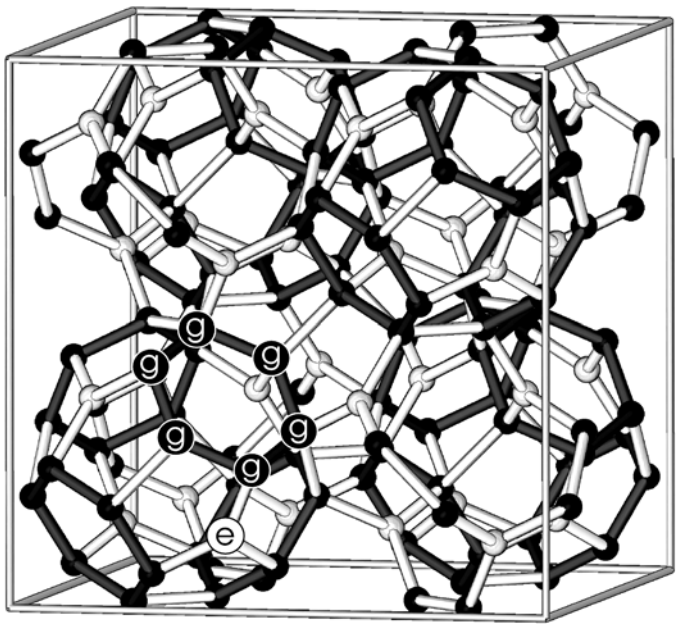

Figure 1. Spatial arrangement of the g- and e-sites in C15 Laves-phase compounds AB_2. Dark spheres: g-sites; bright spheres: e-sites.

the C15 structure and a lattice parameter of $a_0 = (8.095 \pm 0.005)$ Å. The existence of the pure C15 Laves-phase has been reported previously for the concentration range $4.0 \leqslant x \leqslant 4.5$, and it is at least the main phase in Hf Ti_2H_x over the rather wide range $2.0 \leqslant x \leqslant 5.5$ [8]. Figure 2 shows the present data of the lattice parameter together with a_0 values of the C15 phase in other Hf Ti_2H_x samples with different hydrogen content [8]. Evidently, the lattice parameter of the C15 component is independent of the hydrogen content. It should be noted, however, that for $x \leqslant 3.5$ and for $x \geqslant 5.0$ the x value of Hf Ti_2H_x may differ from the hydrogen concentration in the C15 phase due to the coexistence with other phases. A concentration-independent value of a_0 has also been found in the related hydrogen-stabilized Laves-phase C15-$ZrTi_2H_x$ [7]. In contrast, in Laves-phase compounds with preferential g-site occupation a_0 increases linearly with the hydrogen content. This is illustrated by including in figure 2, as an example, the x dependence of a_0 in C15-ZrV_2H_x [19] and C15-ZrV_2D_x [20].

The NMR measurements were performed with home-built Fourier transform spectrometers using phase-alternating pulse schemes and quadrature detection. The sample temperature was maintained to about ± 0.2 K by means of a digital PID controller combined with ohmic heating, and was monitored independently by two Pt–PtRh thermocouples (high-temperature PFG measurements), two Cu–NiCu thermocouples (low-temperature PFG measurements), or by two calibrated platinum resistors (Γ_1 measurements). Temperatures below room temperature were achieved by cooling with cold nitrogen gas (PFG measurements) or liquid helium (Γ_1 measurements) in a separate cryostat in the room-temperature bore of the superconducting magnet. Γ_1 was measured with an inversion–recovery pulse sequence, or with a saturation–recovery pulse sequence at low temperatures. The relaxation rates were determined at 37.3, 67.7 MHz and in the case of $x = 4.0$ also at 90.0 MHz.

The hydrogen diffusivity was measured between 220 and 500 K with a home-built PFG spectrometer at a resonance frequency of 37.3 MHz. The latest modifications of the PFG

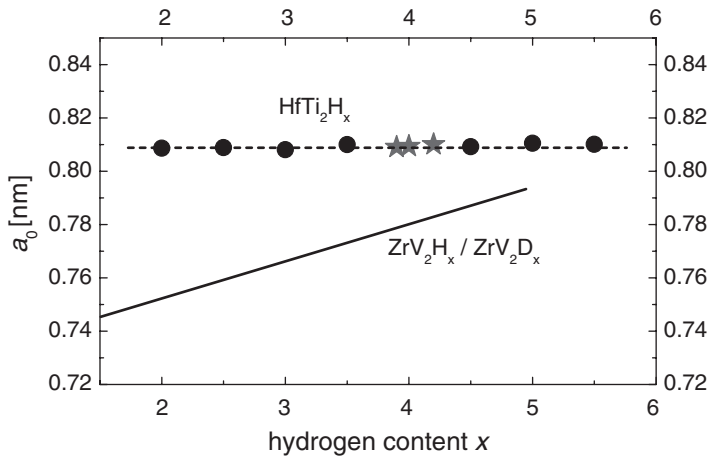

Figure 2. Lattice parameter a_0 of the C15 structure as a function of the hydrogen content. The present results for C15-Hf Ti_2H_x (full stars) are compared with published data (full circles, [8]). Note that for Hf Ti_2H_x with $x \leqslant 3.5$ and $x \geqslant 5.0$ the x value may differ from the hydrogen concentration in the C15 phase. The solid line represents a_0 in C15-ZrV_2H_x and C15-ZrV_2D_x as obtained from [19, 20].

spectrometer at the Max-Planck-Institut für Metallforschung in Stuttgart are described in [21]. The measurements were performed employing the two-pulse spin-echo sequence [12] and, predominately in the range of smaller diffusivities, the stimulated spin-echo sequence [22]. Typical operating conditions were gradient pulse lengths of $\delta = 1$ ms and diffusion times of $\Delta = 3$ ms. The diffusion coefficients D were determined from the dependence of the echo attenuation on the amplitude of the field-gradient pulses, which were varied between 0 and 25 T m^{-1}. The accuracy of a PFG experiment may, in principle, be affected by the presence of magnetic field gradients due to a random variation of the magnetization in powdered metal hydride samples. If such a random variation of the magnetization is present in a sample, a correct measurement of the diffusivity requires alternating pulsed field gradients (APFG) in order to eliminate contributions from the cross term between the applied gradients and the random background gradients. APFG measurements using the spin-echo sequence introduced by Karlicek and Lowe [23], which are experimentally much more demanding, were performed for comparison. Within the experimental uncertainty the APFG measurements yielded exactly the same results as those measured with unipolar pulsed field gradients. Thus, a very high accuracy could also be achieved by using the two-pulse spin-echo or the stimulated spin-echo sequence.

3. Results and discussion

3.1. PFG results

Figure 3 shows the hydrogen diffusivities in C15-Hf Ti_2H_x ($x = 3.9$, 4.0 and 4.2) measured by PFG-NMR. The reproducibility of the data has been confirmed by going through several temperature cycles using different sets of values of δ and Δ. Moreover, diffusion measurements performed by using different pulse sequences yield exactly the same results. Especially, we like to emphasize that the diffusivities obtained by applying APFGs agree with those data measured with the two-pulse or stimulated spin-echo sequence using unipolar gradient pulses.

Table 1. Diffusion parameters of hydrogen in C15-Hf Ti_2H_x obtained by fitting Arrhenius expressions to the diffusivities measured by PFG-NMR over the entire temperature range (220–500 K). The diffusivities at 300 K, D(300 K), have been calculated from the fitting parameters.

x	D_0 (10^{-8} m^2 s^{-1})	H_a (meV)	D(300 K) (10^{-12} m^2 s^{-1})
3.9	3.5 ± 0.5	240 ± 10	3.1
4.0	1.2 ± 0.3	210 ± 10	3.6
4.2	3.4 ± 0.5	235 ± 10	3.8

This is evident from figure 3, where APFG results are included for $x = 3.9$ between 250 and 500 K. Obviously, the background field gradients caused by an inhomogeneous magnetization of the particles in the powdered samples are negligible. From this we conclude that the upper limit for a systematic error in D is well below the statistical uncertainty of typically 10% for APFG-measurements. The solid lines in figure 3 are obtained by fitting Arrhenius laws

$$D = D_0 \exp(-H_a/k_B T) \tag{1}$$

to the diffusion coefficients. The corresponding activation enthalpies H_a and pre-exponential factors D_0 are given in table 1, together with the diffusivities at 300 K. These data are quite similar to those obtained for the related system C15-$ZrTi_2H_x$. PFG measurements on C15-$ZrTi_2H_{3.7}$ [14] yielded $D(300\ \text{K}) = 3.6 \times 10^{-12}$ m^2 s^{-1} and the diffusion parameters $H_a = 0.22$ eV and $D_0 = 1.8 \times 10^{-8}$ m^2 s^{-1}.

Figure 3 shows that over the entire temperature range the temperature dependence of D at a fixed concentration x is quite well represented by an Arrhenius law. A more or less single Arrhenius behaviour of the diffusion coefficient over three orders of magnitude is quite remarkable considering that one expects multiple jump possibilities for hydrogen in C15-Hf Ti_2H_x. This behaviour indicates that the diffusion process is always dominated by a single energy barrier. The observation of a single activation enthalpy for long-range diffusion is compatible with the diffusion mechanism proposed by Skripov and co-workers [18]. In this model, the energy barrier for long-range diffusion is that required to excite a hydrogen atom from an e-site into a g-site (see below). Similar behaviour occurs in other Laves-phase hydrides with g- and e-site occupancy, such as C15-ZrV_2H_x for $x \geqslant 2.5$ [6]. A single Arrhenius law has also been found for $D(T)$ of hydrogen in the lanthanum dihydride–trihydride system LaH_x ($2.0 \leqslant x \leqslant 3.0$), where again two types of occupied sites, i.e. tetrahedral and octahedral interstitial sites, are involved in each jump process contributing to long-range diffusion [24].

Closer inspection of the Arrhenius plots in figure 3 reveals very small but systematic deviations from straight lines. The slopes are, especially in the case of $x = 3.9$, slightly smaller at low temperatures than at high temperatures. The diffusion parameters obtained by fitting equation (1) only to the diffusivities measured between 220 and 350 K are given in table 2, together with results deduced from the relaxation data in more or less the same temperature range. The corresponding H_a values are between 5 and 20% smaller than those obtained by fitting over the entire temperature range (cf table 1). The relationship between D, the effective jump length L and the mean dwell time τ^{diff} between jumps contributing to long-range diffusion is given by

$$D = f^T \frac{L^2}{6\tau^{\text{diff}}} \tag{2}$$

where f^T is the concentration-dependent tracer correlation factor. Neutron scattering data on C15-Hf Ti_2H_x [18] indicate an increase in L with increasing temperature, which may explain the slight deviation from Arrhenius behaviour of $D(T)$.

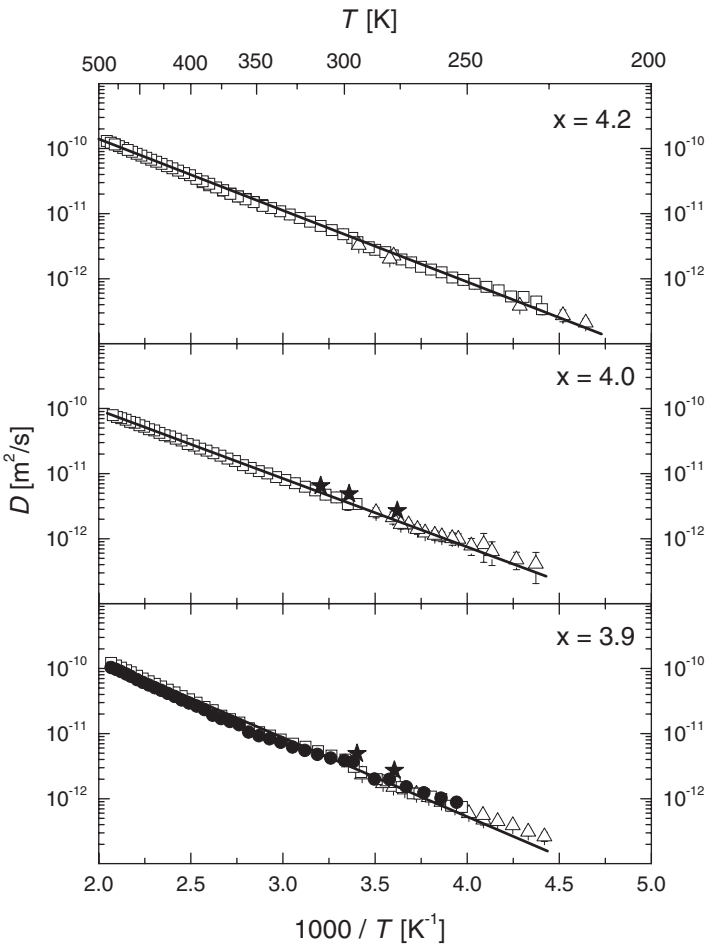

Figure 3. Temperature dependence of the hydrogen diffusivity in C15-Hf Ti_2H_x ($x = 3.9$, 4.0 and 4.2) measured by PFG-NMR with different pulse sequences: two-pulse spin-echo [12] (open squares), stimulated spin-echo [22] (open triangles) and APFG sequence [23] (full circles). The stars denote diffusivities calculated from the Γ_1 data (see text). The solid lines are obtained by fitting Arrhenius expressions $D = D_0 \cdot \exp(-H_a/k_B T)$ to the diffusion coefficients. The corresponding diffusion parameters are summarized in table 1.

Table 2. D_0 and H_a values obtained by fitting Arrhenius expressions to the PFG data measured at low temperatures (220–350 K). τ_0^{diff}, H_a^{diff}, τ_0^{local} and H_a^{local} are the diffusion parameters deduced from the Γ_{1d} data within about the same temperature range. These parameters have been obtained by fitting equation (6) to the dipolar relaxation, using the Sholl model [27] for $\Gamma_{1d}^{\text{diff}}$ related to long-range diffusion and the six-site model [30] for $\Gamma_{1d}^{\text{local}}$ due to localized motion. The corresponding fitting curves are shown as solid lines in figures 4 and 6.

x	D_0 (10^{-8} m^2 s^{-1})	H_a (meV)	τ_0^{diff} (10^{-13} s)	H_a^{diff} (meV)	τ_0^{local} (10^{-11} s)	H_a^{local} (meV)
3.9	0.8 ± 0.3	200 ± 8	4.9 ± 1.0	200 ± 10	3.5 ± 1.0	75 ± 10
4.0	0.8 ± 0.3	200 ± 8	5.0 ± 1.0	200 ± 10	5.5 ± 1.0	65 ± 10
4.2	1.7 ± 0.4	215 ± 8	4.7 ± 1.0	200 ± 10	4.1 ± 1.0	72 ± 10

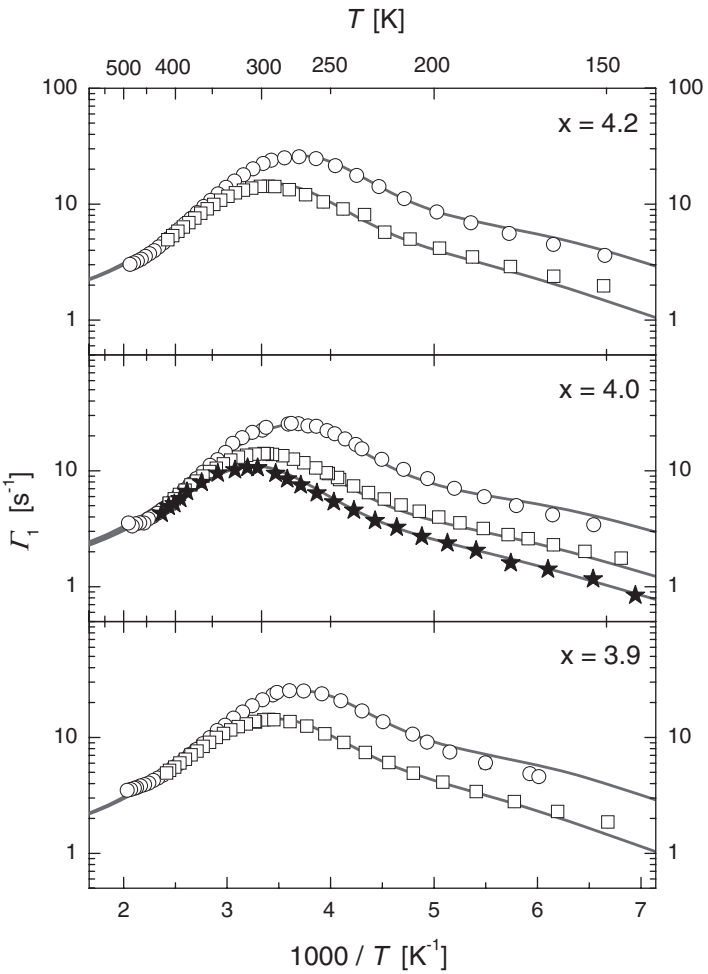

Figure 4. Spin–lattice relaxation rate Γ_1 of hydrogen in C15-Hf Ti_2H_x ($x = 3.9$, 4.0 and 4.2) measured at 37.3 MHz (open circles), 67.7 MHz (open squares) and 90.0 MHz (stars). The sum of Γ_{1e} and Γ_{1d}, with Γ_{1d} consisting of two contributions due to long-range diffusion ($\Gamma_{1d}^{\mathrm{diff}}$) *and* due to localized motion ($\Gamma_{1d}^{\mathrm{local}}$), is represented by solid lines (see text).

3.2. Spin–lattice relaxation

In order to further analyse the mechanisms of hydrogen motion on an atomistic scale, Γ_1-measurements have also been performed on the same samples. Figure 4 shows the temperature dependence of the proton Γ_1 measured at different resonance frequencies. In metallic systems the relaxation rate may be decomposed according to

$$\Gamma_1 = \Gamma_{1e} + \Gamma_{1d}. \tag{3}$$

The electronic contribution Γ_{1e} is due to the interaction between the magnetic moments of the protons and the conduction electrons, and it is usually expressed by the Korringa relation

$$\Gamma_{1e} = T/\kappa \tag{4}$$

with a temperature-independent Korringa constant κ [25]. In order to proof the Korringa law at low temperatures, where the dipolar contribution to Γ_1 is expected to be negligible, the proton

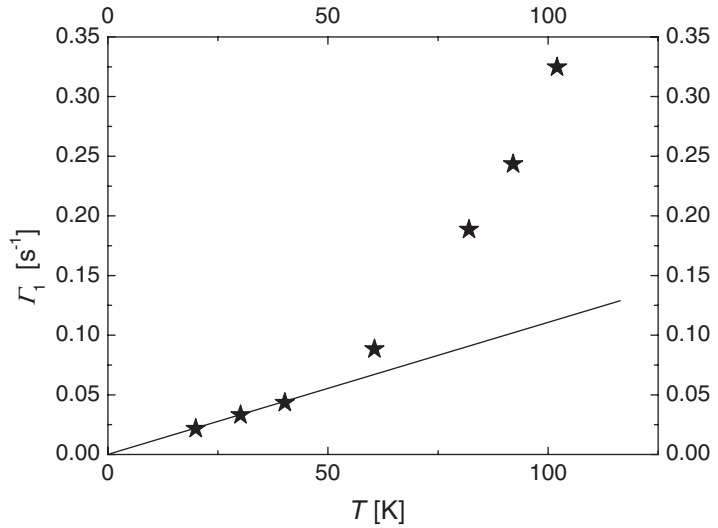

Figure 5. Spin–lattice relaxation rate Γ_1 of hydrogen in C15-Hf$Ti_2H_{4.0}$ measured at 90.0 MHz. The solid line represents the electronic contribution Γ_{1e} with the Korringa product $\kappa = 913$ K s.

Γ_1 measured on C15-Hf$Ti_2H_{4.0}$ at $\omega/2\pi = 90.0$ MHz is plotted in figure 5 on a linear scale versus the temperature T. The straight line in figure 5 is obtained by fitting equation (4) to the data below about 40 K and it corresponds to $\kappa = 913$ K s. In this temperature range, the Γ_1 data show pure Korringa behaviour, but already at about 50 K Γ_1 starts to deviate from the Korringa law. This indicates a significant dipolar contribution Γ_{1d} even at temperatures well below the relaxation maximum.

Γ_{1d} is due to the magnetic dipole–dipole interaction of a given proton with neighbouring protons and, in general, also with the host nuclei. In the case of HfTi_2H_x ($3.9 \leqslant x \leqslant 4.2$), Γ_{1d} is dominated by the dipole–dipole interaction between the protons. In this case, the correlation time of the proton–proton interaction is given by $\tau_c = \tau/2$, if τ is the mean dwell time after which one of the two interacting protons jumps.

According to neutron scattering data [18], hydrogen motion occurs on two different timescales in C15-HfTi_2H_x: since the site energy of the g-sites is higher than that of the e-sites, the e-sites are preferably occupied. It is evident from the spatial arrangement of the interstitial sites in the C15 lattice (see figure 1) that a transition from one e-site to another one occurs via at least two intermediate g-sites. Thus, a hydrogen atom participating in the long-range diffusion jumps out of the e-site sublattice and performs a number of jumps on a hexagon formed by six g-sites before it finds a vacant e-site. The jumps on the g-site hexagons occur on a faster time scale, resulting in the fast localized motion. For this jump model the two different time scales of hydrogen motion are given by the mean residence time τ^{local} of a hydrogen atom at a certain g-site, and the average time τ^{diff} spent by a hydrogen atom on the g-site sublattice before it finds a vacant e-site. Only the transitions from one e-site to another one, which occur after $\tau^{\mathrm{diff}} \gg \tau^{\mathrm{local}}$, contribute to the long-range diffusion, but both dynamical processes contribute to Γ_{1d}.

3.3. Long-range diffusion

In order to analyse the relaxation data in terms of hydrogen diffusion, a relaxation model is required that takes into account the structure of the hydrogen sublattice. It is often assumed [17]

that the e-sites form a face-centred cubic (fcc) lattice with lattice parameter $a_0/2$. However, this is only correct if the positional parameter X_e of hydrogen at an e-site is equal to 0.25. Neutron diffraction experiments on C15-Hf Ti_2D_4 revealed $X_e = 0.267$ [10]. This means that hydrogen atoms occupying e-sites are displaced from their positions in the ideal fcc sublattice, resulting in a change of the distances between the e-sites. Out of the twelve nearest-neighbour e-site three are closer and three are further away than in the case of the ideal fcc sublattice. The distances between neighbouring e-sites in C15-Hf Ti_2D_4 are 2.47, 2.87 and 3.25 Å [10]. Since the overall fcc symmetry is maintained, it is a reasonable approximation to analyse the spin–lattice relaxation due to translational diffusion by Monte Carlo-calculations for jumps between nearest-neighbour sites on a fcc lattice [26,27]. Analytic representations of the Monte Carlo-calculations, that depend slightly on the occupation probability of a site in the fcc lattice c_e, are given in [27] and yield spin–lattice relaxation rates as a function of the mean dwell time τ^{diff}. The calculations for $c_e = 0.99$ and 1.0 have been used to analyse the relaxation data of the samples with $x < 4$ and $x \geqslant 4$, respectively. Furthermore, a thermally activated process of long-range diffusion according to

$$\tau^{diff} = \tau_0^{diff} \cdot \exp(H_a^{diff}/k_B T) \tag{5}$$

is assumed. This approach is capable of describing the Γ_{1d} data very well between about 250 and 350 K, where contributions to Γ_{1d} due to localized motion are expected to be negligible.

Using [27] with $c_e = 0.99$ and 1.0 for $x = 3.9$ and 4.0, respectively, the value of τ^{diff} at the temperature of the relaxation rate maximum, T_{max}, can be estimated from $\tau^{diff} = 0.93/\omega$, where $\omega/2\pi$ is the NMR frequency. For hopping on an fcc lattice with $c_e = 0.99$ and 1.0 the tracer correlation factors $f^T = 0.781$ and 0.789 have been calculated by Sankey and Fedders [28]. The diffusivities calculated from equation (2) by using an average jump distance between neighbouring e-sites of $L = a_0/\sqrt{8} \approx 2.87$ Å, are included in figure 3. They are only slightly higher than the diffusivities measured directly by PFG-NMR. This is consistent with the assumption that the main Γ_{1d} peak is, indeed, related to long-range diffusion of hydrogen in Hf Ti_2H_x. In the case of C15-$ZrTi_2H_x$, the diffusivities deduced from the Γ_{1d} data as outlined above were also slightly but systematically higher than the PFG results [14]. This may indicate that the average jump distance of hydrogen atoms is about 2.5 Å and thus somewhat smaller than assumed. On the other hand, it cannot be excluded that the deviations are related to the finite g-site occupancy, which has not been taken into account in the relaxation model.

3.4. Localized motion

Figure 6 shows the Γ_1 data of hydrogen in C15-Hf $Ti_2H_{4.0}$ measured at 37.3 MHz. The thin solid curve indicates the electronic contribution and the dashed curve represents the dipolar relaxation due to long-range diffusion. A comparison with the experimental data gives clear evidence that at low temperatures additional contributions to Γ_1 occur, which are most likely related to localized motion. Thus, Γ_{1d} may be written as

$$\Gamma_{1d} = \Gamma_{1d}^{diff} + \Gamma_{1d}^{local} \tag{6}$$

where Γ_{1d}^{diff} and Γ_{1d}^{local} denote the dipolar relaxation rates caused by long-range diffusion and by localized motion, respectively. A similar feature has been observed for hydrogen in C15-$ZrTi_2H_x$, where the Γ_{1d}^{local} data have been interpreted in terms of a broad distribution of the activation enthalpies for localized motion [17]. It turns out that also in the present case the low-temperature contributions to Γ_{1d}^{local} cannot be described satisfactorily by a single BPP formula [29] with a fixed activation enthalpy. A description of the experimental data is again possible under the assumption of a distribution of the activation

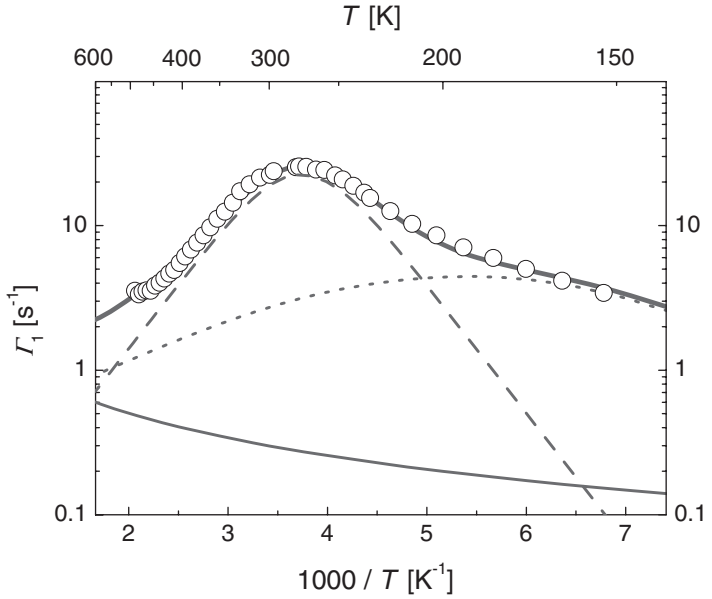

Figure 6. Γ_1 data of hydrogen in C15-Hf$Ti_2H_{4.0}$ measured at 37.3 MHz. The thin solid line represents the electronic relaxation Γ_{1e} with the Korringa product $\kappa = 913$ K s. The dipolar spin–lattice relaxation consists of two contributions, $\Gamma_{1d}^{\text{diff}}$ and $\Gamma_{1d}^{\text{local}}$, which are due to long-range diffusion and due to localized motion. $\Gamma_{1d}^{\text{diff}}$ is represented by the dashed line (Sholl's model [27] for long-range diffusion) and $\Gamma_{1d}^{\text{local}}$ by the dotted line (six-site model [30] for localized motion). The sum of the three contributions is given by the bold solid line. The fitting parameters are included in table 2.

enthalpies for localized motion according to

$$\Gamma_{1d}^{\text{local}} = \int_0^\infty \Gamma_{1d}(\tau_0^{\text{local}}, H_a^{\text{local}}) G(H_a^{\text{local}})\, \mathrm{d}H_a^{\text{local}} \tag{7}$$

where $\Gamma_{1d}(H_a^{\text{local}})$ is the relaxation rate obtained by the phenomenological BPP model [29]. The $\Gamma_{1d}^{\text{local}}$ data between about 50 and 200 K can be fitted quite well using equation (7) with a constant prefactor τ_0^{local} and a Gaussian distribution function

$$G(H_a^{\text{local}}) = \exp[-(H_a^{\text{local}} - \overline{H_a}^{\text{local}})^2 / 2\Delta H_a^{\text{local}2}] \tag{8}$$

for the activation enthaply. Typical values for the fits (which are not shown) are $\tau_0^{\text{local}} \approx 10^{-11}$ s, $\overline{H_a}^{\text{local}} \approx 100$ meV and $\Delta H_a^{\text{local}} \approx 20$ meV. Owing to the large number of fitting parameters, different values can be obtained within certain limits. But in any case, the analysis using equations (7) and (8) yields a surprisingly large distribution width $\Delta H_a^{\text{local}}$. One may imagine that the activation enthalpy of localized motion is changed if more than one hydrogen atom is occupying a g-site hexagon, and H_a^{local} may also depend on the number of occupied e-sites in the vicinity. Nevertheless, such wide distributions cannot be understood for a crystalline compound.

A more adequate approach to describe $\Gamma_{1d}^{\text{local}}$ caused by localized motion on the g-site hexagons is obtained under the following assumptions: for an occupation probability of a given g-site in HfTi_2H_x ($3.9 \leqslant x \leqslant 4.2$) of about $c_g = 0.07$ (even smaller c_g values are found below room temperature [10]), the likelihood of having two or more hydrogen atoms per hexagon is only about 0.08. Thus, in a good approximation, it may be assumed that a

hydrogen atom within a hexagon is only interacting with neighbouring hydrogen atoms on e-sites. If one further assumes that e-site hydrogen is immobile on the time scale of localized motion, the corresponding pair correlation function for dipole–dipole interaction may be easily calculated. It is essentially given by a one-particle correlation function as required to analyse QENS data. The case of a hydrogen atom jumping between neighbouring sites on a hexagon is considered in the so-called six-site model [30], which yields a correlation function

$$g(t) = \sum_{j=1}^{3} a_j \exp(-\tau_i/t) \tag{9}$$

that consists of three exponential terms with $\tau_1 = \tau^{\text{local}}/0.5$, $\tau_2 = \tau^{\text{local}}/1.5$, $\tau_3 = \tau^{\text{local}}/2$. The ratio of the prefactors in equation (9) is given by $a_1{:}a_2{:}a_3 = 2{:}2{:}1$. This correlation function results in a spectral density function consisting of three Lorentzian curves (BPP-type curves). The relaxation model based on equation (9) is capable of describing $\Gamma_{1d}^{\text{local}}$ caused by localized motion very well. The agreement of the six-site model with the experimental data is, even without assuming a distribution of activation enthalpies and thus with one fitting parameter less, at least as good as that obtained by using equations (7) and (8). A fit of the Γ_1 data of hydrogen in C15-Hf $Ti_2H_{4.0}$ measured at 37.3 MHz is shown in figure 6. The thick solid curve represents the sum of the electronic contribution Γ_{1e}, the dipolar contribution due to long-range diffusion $\Gamma_{1d}^{\text{diff}}$ (Sholl model), and the dipolar contribution due to localized motion $\Gamma_{1d}^{\text{local}}$ (six-site model). The corresponding fitting parameters are given in table 2. Besides the data shown in figure 6, also the Γ_1 data measured at other NMR frequencies are well represented by these parameters (cf figure 4). For all three samples, the $\Gamma_1(T, \omega)$ data have been analysed in this way. The obtained fitting curves are shown as solid lines in figure 4, and the fitting parameters are summarized in table 2. The H_a^{diff} values are in excellent agreement with the activation enthalpies H_a deduced from the PFG data in the same temperature range, confirming that H_a^{diff} is indeed the activation enthalpy for long-range diffusion. The activation enthalpies obtained by fitting only Sholl's model to the Γ_{1d} data between 250 and 350 K yields activation enthalpies that are slightly smaller than the H_a^{diff} values given in table 2. Together with the results shown in figure 5, this indicates that the spin–lattice relaxation is affected by the localized motion over a fairly wide temperature range of about 50–300 K.

4. Summary and conclusions

The PFG-NMR allowed us to study the long-range diffusivity of hydrogen in the hydrogen-stabilized compound C15-Hf Ti_2H_x over three orders of magnitude. The activation enthalpies obtained by fitting Arrhenius terms to the diffusivities, 240 meV ($x = 3.9$), 210 meV ($x = 4.0$) and 235 meV ($x = 4.2$), change only slightly with the concentration x. Measurements of the spin–lattice relaxation rate indicate that in addition to long-range diffusion localized motion occurs on a faster timescale. The present data are consistent with a model of hydrogen motion, which has been proposed previously on the basis of neutron scattering results [18]: long-range diffusion occurs by jumps from one e-site via intermediate g-sites to another e-site. These jumps take place after a mean dwell time τ^{diff} and the effective activation enthalpy is that required to excite a hydrogen atom from an e-site into a g-site. While being located at the g-site sublattice, the hydrogen atoms contribute to localized motion by jumps between six g-sites forming a hexagon. The mean residence time at a g-site within a hexagon is given by τ^{local}, which is substantially shorter than τ^{diff}. The dipolar contribution to the spin–lattice relaxation can be explained consistently by using Sholl's model for long-range diffusion via e-sites and the six-site model for localized motion on the g-sites. It should be emphasized that this

approach is capable of describing the data without assuming a wide distribution of the activation enthalpies. The activation enthalpies deduced from the Γ_{1d} data are about $H_a^{\mathrm{diff}} \approx 200$ meV for long-range diffusion and $H_a^{\mathrm{local}} \approx 70$ meV for localized motion. The H_a^{diff} values are in excellent agreement with the activation enthalpies determined by the temperature dependence of the long-range diffusivity measured by PFG-NMR.

Acknowledgments

This work was supported by the Deutsche Forschungsgemeinschaft (Project MA 1382/1) and by the Russian Foundation for Basic Research (grant no 99-02-16311). AVS is grateful to the Alexander von Humboldt Foundation for financial support.

References

[1] Skripov A V, Cook J C, Sibirtsev D S, Karmonik C and Hempelmann R 1998 *J. Phys.: Condens. Matter* **10** 1787
[2] Skripov A V, Pionke M, Randl O and Hempelmann R 1999 *J. Phys.: Condens. Matter* **11** 1489
[3] Skripov A V, Cook J C, Karmonik C and Kozhanov V N 1999 *Phys. Rev.* B **60** 7238
[4] Somenkov V A and Irodova A V 1984 *J. Less-Common Met.* **101** 481
[5] Yvon K and Fischer P 1988 *Hydrogen in Intermetallic Compounds* vol 1, ed L Schlapbach (Berlin: Springer) p 87
[6] Majer G, Kaess U, Stoll M, Barnes R G and Shinar J 1997 *Diffus. Defect Data, Solid State Data* A **143–147** 957
[7] Miron N F, Shcherbak V I, Bykov V N and Levdik V A 1971 *Sov. Phys.–Crystallogr.* **16** 266
[8] Kozhanov V N, Skripov A V, Romanov E P 1998 *J. Alloys Compd.* **269** 141
[9] Skripov A V, Udovic T J, Huang Q, Cook J C and Kozhanov V N 2000 *J. Alloys Compd.* **311** 234
[10] Fischer P, Fauth F, Böttger G, Skripov A V and Kozhanov V N 1999 *J. Alloys Compd.* **282** 184
[11] Barnes R G 1997 *Hydrogen in Metals III* ed H Wipf (Berlin: Springer) p 93
[12] Stejskal E O and Tanner J E 1965 *J. Chem. Phys.* **42** 288
[13] Renz W, Majer G, Seeger A and Skripov A V 1994 *J. Phys.: Condens. Matter* **6** 6367
[14] Renz W, Majer G and Skripov A V 1995 *J. Alloys Compd.* **224** 127
[15] Majer G, Renz W, Seeger A, Barnes R G, Shinar J and Skripov A V 1995 *J. Alloys Compd.* **231** 220
[16] Majer G 1998 *Mater. Res. Soc. Symp. Proc.* **513** 109
[17] Skripov A V, Rychkova S V, Belyaev M Yu and Stepanov A P 1989 *Solid State Commun.* **71** 1119
[18] Skripov A V, Combet J, Grimm H, Hempelmann R and Kozhanov V N 2000 *J. Phys.: Condens. Matter* **12** 3313
[19] Skripov A V, Belyaev M Yu, Rychkova S V and Stepanov A P 1991 *J. Phys.: Condens. Matter* **3** 6277
[20] Eberle U and Majer G 2001 unpublished data
[21] Galvosas P, Stallmach F, Seiffert G, Kärger J, Kaess U and Majer G 2001 *J. Magn. Reson.* **151** 260
[22] Tanner J E 1970 *J. Chem. Phys.* **52** 2523
[23] Karlicek Jr R F and Lowe I J 1980 *J. Magn. Reson.* **37** 75
[24] Majer G, Kaess U and Barnes R G 1999 *Phys. Rev. Lett.* **83** 340
[25] Korringa J 1950 *Physica* **16** 601
[26] Faux D A, Ross D K and Sholl C A 1986 *J. Phys. C: Solid State Phys.* **19** 4115
[27] Sholl C A 1988 *J. Phys. C: Solid State Phys.* **21** 319
[28] Sankey O F and Fedders P A 1979 *Phys. Rev.* B **20** 39
[29] Bloembergen N, Purcell E M and Pound R M 1948 *Phys. Rev.* **73** 679
[30] Bée M 1988 *Quasielastic Neutron Scattering* (Bristol: Adam Hilger)